Available online at www.sciencedirect.com
SCIENCE DIRECT®
Journal of Solid State Chemistry 178 (2005) 3210–3215
JOURNAL OF SOLID STATE CHEMISTRY
www.elsevier.com/locate/jssc

Rapid communication

The effect of hydrothermal growth temperature on preparation and photoelectrochemical performance of ZnO nanorod array films

Min Guo[a,b,*], Peng Diao[c], Xindong Wang[a], Shengmin Cai[b]

[a]*Department of Physical Chemistry, University of Science and Technology Beijing, Beijing 100083, PR China*
[b]*College of Chemistry and Molecular Engineering, Peking University, Beijing 100871, PR China*
[c]*Department of Applied Chemistry, School of Materials Science and Engineering, Beihang University, Beijing 100083, PR China*

Received 26 May 2005; received in revised form 18 July 2005; accepted 19 July 2005
Available online 24 August 2005

Abstract

Highly oriented ZnO nanorod arrays with controlled diameter and length, narrow size distribution and high orientation consistency have been successfully prepared on ITO substrates at different growth temperatures by using a simple hydrothermal method. XRD results indicate that the nanorods are high-quality single crystals growing along [001] direction with a high consistent orientation perpendicular to the substrate. SEM images show that the nanorods have average diameters of about 30–70 nm by changing growth temperature. The thin films consisting of ZnO nanorods with controlled orientation onto ITO substrates allow a more efficient transport and collection of photogenerated electrons through a designed path. For a sandwich-type cell, the relatively high overall solar energy conversion efficiency reaches about 2.4% when the growth temperature is at 95 °C.

Keywords: ZnO nanorod arrays; Photoelectrochemical properties; Hydrothermal; Growth temperature

1. Introduction

As the ordered ZnO nanostructure has been envisioned to enhance performance of various technologically important devices such as short-wavelength lasers [1], Grätzel-type solar cell [2,3], and chemical sensors [4,5], the interest in synthesis of well-aligned ZnO nanowires or nanorods on substrates keeps growing. Perpendicularly oriented single-crystalline ZnO nanorod arrays have been recently fabricated on sapphire substrates using VLS [1] and CVD methods [6,7]. However, these methods involve complex procedures, sophisticated equipment and high temperature ($\geqslant$890 °C for VLS [1] and 500 °C for CVD methods [6,7]). Wet chemical approaches to well-aligned ZnO nanorod arrays on substrates are attracting considerable research activities because of their low growth temperatures and good potential for scale-up. In this regard, O'Brien et al. [8] reported the growth of ZnO nanocolumns with an average diameter of about 532 nm from aqueous solution on fluorine-doped tin oxide glass substrates that were coated with ~20 nm gold layer. Boyle et al. [9] developed a two-step approach, which involves a pre-coating step of ZnO template layer and a subsequent solution deposition process, to produce perpendicularly oriented ZnO submicrorods. Imai and Yamabi [10] studied the essential conditions for the growth of wurtzite ZnO films in aqueous solution by changing pH and complex agent, and also obtained arrayed ZnO nanorod on modified substrates. Vayssieres et al. [11] prepared ZnO nanorods with diameter of 200 nm by hydrothermal method, and very recently, a two-step growth process was used to synthesize ZnO nanowires from aqueous solution by Yang's group [12]. However, for many

*Corresponding author. Department of Physical Chemistry, University of Science and Technology Beijing, Beijing 100083, PR China. Fax: +86 10 62332651.
E-mail address: guomin@metall.ustb.edu.cn (M. Guo).

0022-4596/$ - see front matter © 2005 Elsevier Inc. All rights reserved.
doi:10.1016/j.jssc.2005.07.013

practical applications, it still remains a great challenge to fabricate large-area, well-aligned single-crystalline ZnO nanorods with controlled diameter and length, narrow size distribution and high orientation consistency by using a simple low-cost and low-temperature method.

On the other hand, as we know that zinc oxide is a wide bandgap semiconductor which is one of the ideal materials to be used as electrodes for dye-sensitized solar cells [3]. Nanostructured ZnO electrodes based on interconnected spherical particles have shown low photocurrent efficiency due to charge-carrier recombination losses at grain boundaries between the nanoparticles in the film [13]. A desirable morphology of the thin film should have the channels parallel to each other and vertically with respect to the substrate such as nanorod/tube arrays [13]. Superior photo-to-electric performance of such oriented films is promising.

In this paper, low-temperature growth of well-aligned ZnO nanorod arrays on ITO substrates at different growth temperatures is investigated under hydrothermal conditions. Diameter- and length-controlled growth of ZnO nanorod arrays, with average diameter smaller than 70 nm, in narrow size distribution and high orientation consistency from zinc nitrate aqueous solution are achieved in large scale by adjusting the growth temperature. When employed as photoanodes in dye-sensitized solar cells, the ZnO nanorod array films show relatively higher photoconversion efficiency.

2. Experimental

2.1. Materials

All chemicals (Beijing Chemicals Co. Ltd.) were of analytical reagent grade and used without further purification. All the aqueous solutions were prepared using double distilled and ion-exchanged water. Indium tin oxide (ITO, $10\,\Omega/cm^2$) glass plates were used as substrates and were cleaned by standard procedures prior to use.

2.2. Preparation and characterization of ZnO nanorod array films [14]

ZnO nanorod array films were synthesized from zinc nitrate in a neutral aqueous solution under hydrothermal conditions. The procedure consists of two steps: (1) modification of ITO substrates with a thin layer of densely and uniformly dispersed ZnO nanoparticles by spin coating, and (2) hydrothermal growth of ZnO nanorods in aqueous solution. In detail, zinc acetate dihydrate ($Zn(CH_3COO)_2 \cdot 2H_2O$) was dissolved in the mixed solution of ethanolamine ($NH_2CH_2CH_2OH$) and 2-methoxyethanol ($CH_3OCH_2CH_2OH$). The concentrations of both $Zn(CH_3COO)_2$ and ethanolamine in the resulting solution are 0.75 M. The resulting mixture was then agitated at 60 °C for 30 min to yield a homogeneous and stable colloid solution, which served as coating solution. The coating colloid solution (~2 mL) was dropped onto $1.5 \times 3.0\,cm^2$ ITO substrates for spin coating, then the substrates were dried and annealed at 300 °C for 10 min. More than three cycles were needed for the dense and uniform dispersion of ZnO nanoparticles on ITO substrates. The subsequent hydrothermal growth was carried out at different growth temperatures in a sealed kettle by immersing the modified substrates in the aqueous solution (80 mL) containing $Zn(NO_3)_2$ (0.1 mol/L) and methenamine (0.1 mol/L). Finally, the samples were washed with deionized water and allowed to dry in air before characterization.

The morphology of the nanorods was characterized using scanning electron microscopy (SEM; Philips FEI XL30 SFEG). X-ray diffraction (XRD) analysis was performed with a Rigaku Dmax-2000 diffractometer using Cu$K\alpha$ radiation. The surface area of the ZnO nanorod array films on ITO substrate grown at 95 °C was studied using nitrogen adsorption–desorption apparatus (Model ASAP 2010, Micromeretics Instrument Corp.).

2.3. Photoelectrochemical measurement

Dye sensitization of the ZnO nanorod array films were done by soaking them in 0.5 mmol/L $Ru(dcbpy)_2(NCS)_2$(dcbpy = 4,4′-dicarboxy-2,2′-bipyridine)(N3) for 30 min. Electrodes N3/ZnO/95, N3/ZnO/80, N3/ZnO/60 and N3/ZnO/40 were obtained by immersing ZnO nanorod array films grown on ITO substrates at different temperatures of 95, 80, 60 and 40 °C in the dye solution, respectively. The photoelectrochemical experiments were performed in a sandwich-type two-electrode cells. The dye-coated film was used as working electrode, platinized ITO glass as counter electrodes and 0.3 mol/L LiI + 0.03 mol/L I_2 propylene carbonate (PC) solution as electrolyte. A 150 W Xenon lamp combining a high-intensity grating monochromator (Beijing instrument corporation) served as light source. The photocurrent action spectrum was determined by measuring the short-circuit photocurrent at various excitation wavelengths. In photocurrent–photovoltage measurement, a 10 cm water filter and a 350 nm cut-off filter was placed in the path of the excitation beam. The photoelectric conversion efficiency was calculated with the deduction of light absorption and transmission loss in ITO glass. All the measurements were conducted at room temperature.

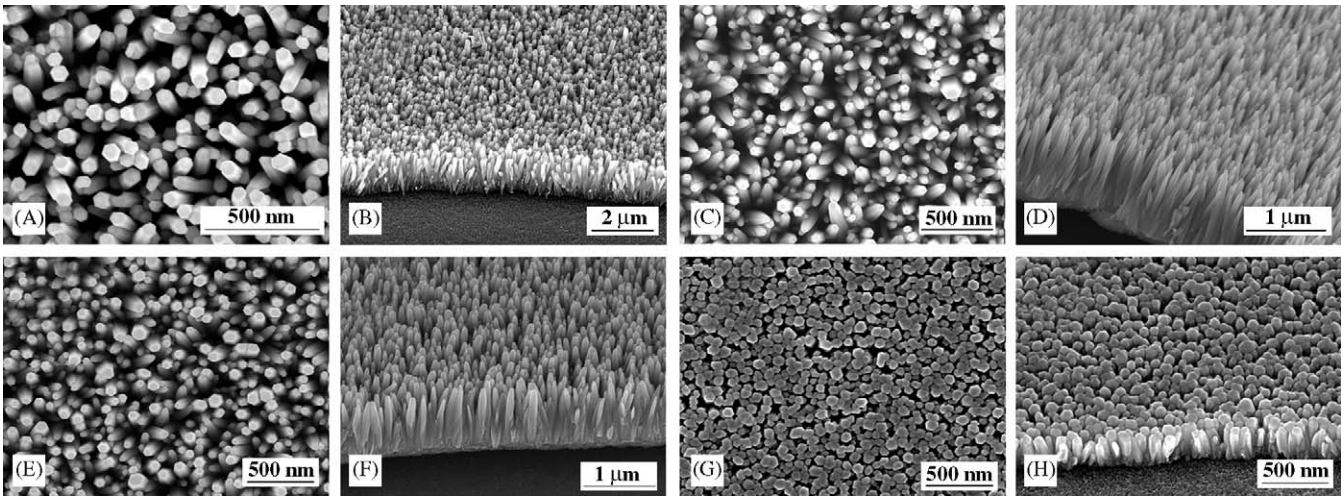

Fig. 1. SEM images of the ZnO nanorod array films grown on ITO substrates from 95 to 40 °C. (A, C, E, G) Top view and (B, D, F, H) view from 45°. Growth time: 4 h.

3. Results and discussions

Fig. 1 illustrates the morphology of ZnO nanorod arrays grown on the modified ITO substrates at different growth temperatures. The morphology of the nanorod arrays is controlled by the temperature of the hydrothermal treatment used for films preparation. The top-view SEM images (Fig. 1A, C, E, G) indicate that well-aligned ZnO nanorods grow uniformly in large scale, and the well-defined crystallographic planes of the hexagonal single-crystalline nanorods can be clearly identified, providing strong evidence that the nanorod arrays grow along the [001] direction. The nanorods diameter distributions obtained from the corresponding SEM images are shown in the histogram in Fig. 2, from which we note that the average diameters of the ZnO nanorods can be controlled at different growth temperatures. When the growth temperature decreased from 95 to 60 °C, the average diameters of the ZnO nanorods decreased from 65 to 30 nm, correspondingly. However, the decreasing trend of the average diameter was not observed as the ZnO nanorods grown at 40 °C. In contrast, the average diameter of the ZnO nanorods grown at 40 °C is about 45 nm. All the average diameters of the ZnO nanorods grown at different temperatures are smaller than 70 nm which is much smaller than that obtained previously [8–11,15,16]. The dispersity of the nanorod width is believed to be caused by the inhomogeneous sizes of ZnO nanoparticles preformed on substrates.

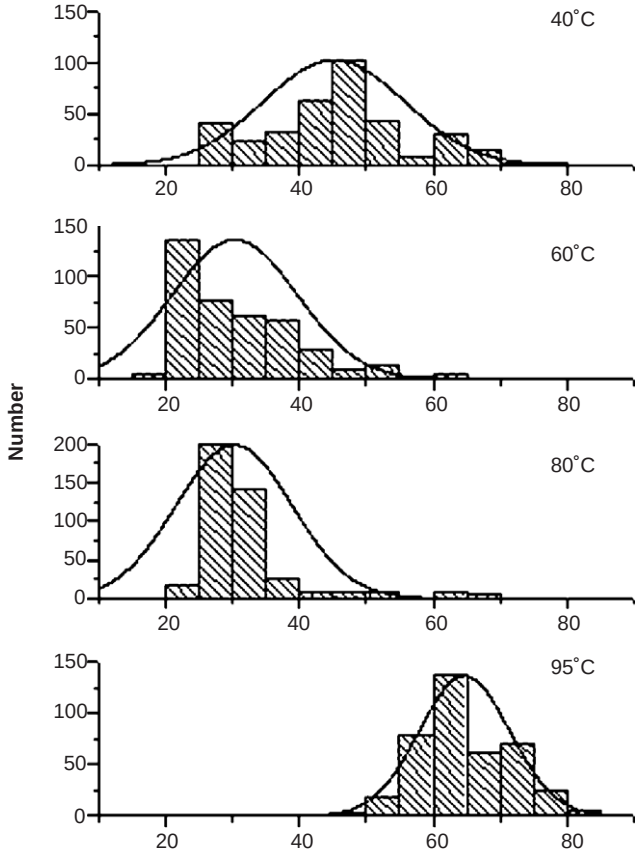

Fig. 2. Effect of temperature on diameter distributions of ZnO nanorods grown on ITO substrates from 95 to 40 °C. Growth time: 4 h.

The cross-section images of as-prepared nanorod arrays are shown in Fig. 1B, D, F and H, from which we note that nearly all the nanorods grow vertically from the substrates. The nanorod lengths can be increased from about 240 to 850 nm, 1.1 and 1.9 μm when the deposition temperature is increased from 40 to 60, 80 and 95 °C. This implies that the growth rate along [001] direction is more sensitive to temperature compared to those along [101] and [100] directions. Therefore, changing the growth temperature is one of the important means to control the length of the nanorod

arrays. The small width and relatively large length results in the relatively high specific area, which is an important parameter in many applications.

The density of the ZnO nanorods is estimated to be about 10^{10} nanorods per square centimeter, and the specific area of the nanorod array films grown at 95 °C is measured to be about $72 \pm 6\,m^2/g$, which is the largest value among that of the four nanorod array films. This implied that the as-prepared ZnO nanorod array films have relatively large surface area which would be beneficial for adsorbing more dyes, when used as photoanode of dye-sensitized solar cell, to improve the light harvest efficiency.

XRD patterns of ZnO nanorods arrays were taken to examine the crystal structure of the nanorods. All samples gave similar XRD patterns indicating the nanorods in high crystallinity. Fig. 3 shows the typical XRD patterns of the well-ordered ZnO nanorods arrays grown on ITO substrate. Only two peaks, which are indexed as 0 0 2 and 0 0 4 of the wurtzite structure of ZnO, are observed, indicating excellent orientation in the *c*-axis direction of these nanorod arrays over a large area. In contrast to the XRD spectra of the ZnO nanorods prepared by using the same hydrothermal method [8–11,15–17], wherein the diffraction peaks of 1 0 0, 1 0 1, 1 0 2, 1 0 3 appeared with the 0 0 2 peaks, the much higher intensity of the 0 0 2 diffraction peak provides further evidence that the nanorod arrays are in high orientation consistency on the substrates in our case which can be compared to that of ZnO nanorods by VLS or CVD mechanism.

Fig. 4 gives the absorption spectra of dye N3 attached onto the ZnO nanorod array films with different film thicknesses after 30 min adsorption. Upon adsorption on ZnO films the spectra of dye N3 have the same maximum values at around 535 nm compared with that

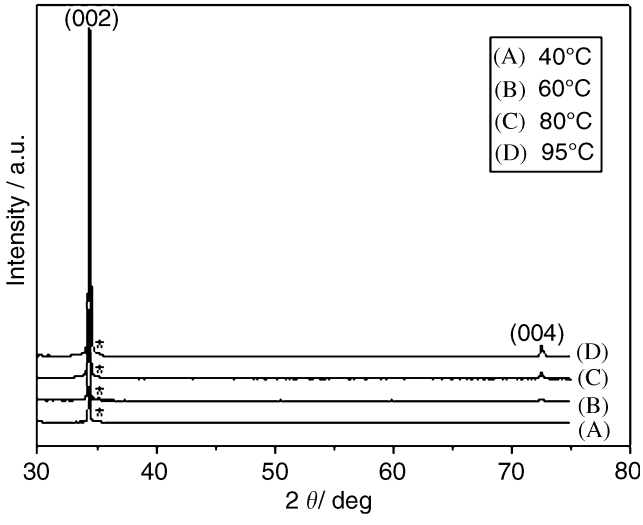

Fig. 3. Effect of temperature on XRD patterns of the ZnO nanorod arrays grown on ITO substrate (*) from 95 to 40 °C. Growth time: 4 h.

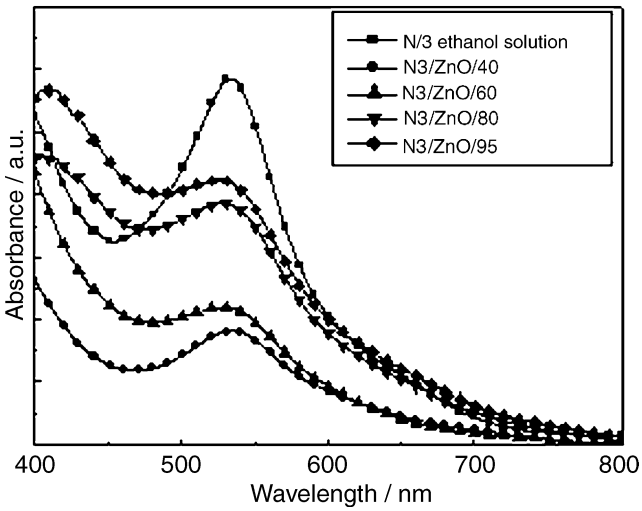

Fig. 4. Absorption spectra of N3 in absolute ethanol solution and absorbed on ZnO nanorod array films grown from 95 to 40 °C.

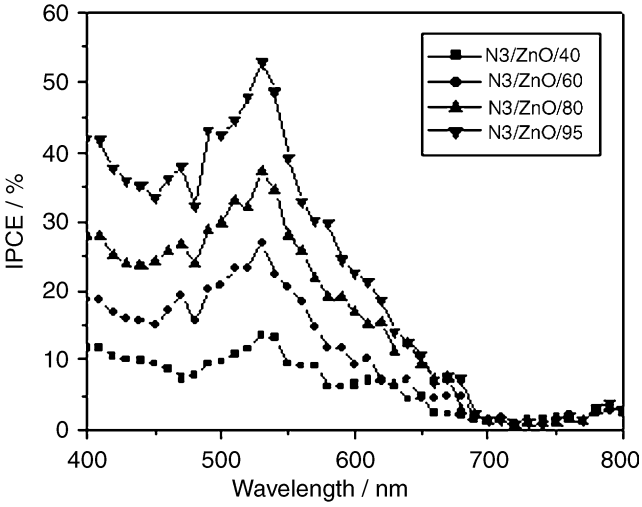

Fig. 5. Photocurrent action spectra of the N3-sensitized ZnO electrodes grown from 95 to 40 °C.

in ethanol solution. From Fig. 4, we can see that the intensities of the absorption peaks of N3 are increasing gradually with increasing thickness of ZnO nanorod arrays, suggesting that more dyes have been adsorbed onto the thicker films than that onto the thinner films. The amount of N3 adsorbed on ZnO films per unit area were measured and the dye N3 attached onto N3/ZnO/95 electrode gives the value of 1.8×10^{-8} mol/cm^2. As for dye N3 attached onto N3/ZnO/80, N3/ZnO/60 and N3/ZnO/40 electrodes, the values decrease from 1.4×10^{-8} to 0.7×10^{-8} and 0.21×10^{-8} mol/cm^2. The data show that the ZnO nanorod array films grown at 95 °C have relatively large surface area which would be beneficial for adsorbing more dyes, when used as photoanode of dye-sensitized solar cell, to improve the light harvest efficiency.

The photocurrent action spectra of the dye-sensitized ZnO nanorod array films grown on ITO substrates at different growth temperatures are shown in Fig. 5. The monochromatic incident photo-to-electric conversion efficiency (IPCE), defined as the number of electrons generated by light in the outer circuit divided by number of incident photons, is represented by the following equation:

$$\mathrm{IPCE}(\%) = 1241 I_{sc}\,(\mu\mathrm{A\,cm^{-2}})/\lambda\,(\mathrm{nm}) P_{in}\,(\mathrm{mW\,cm^{-2}}) \times 100, \quad (1)$$

where I_{sc} is the short-circuit photocurrent density for monochromatic incident light and λ and P_{in} are the wavelength and the intensity of the monochromatic light, respectively. From Fig. 5, we can see that the photocurrent action spectra of the dyes in a dye-sensitized solar cell match their absorption spectra (Fig. 4). The N3/ZnO/95 electrode gives the maximum IPCE performance 52.7% at 535 nm. This value is almost equal to those reported for the combination of colloid-processed ZnO film and N3 [18]. As for N3/ZnO/80, N3/ZnO/60 and N3/ZnO/40 electrodes, the IPCE values decrease from 37.2% to 26.9% and 13.4% at the same wavelength. The relatively low photocurrent for the above-mentioned electrodes compared to that for N3/ZnO/95 electrode may be caused by the decreasing amount of N3 absorbed on the three electrodes, which is attributed to the decreasing thickness of the well-aligned ZnO nanorod array films prepared on the low growth temperatures. The high IPCE values obtained indicate the excellent ability of ZnO electrodes based on nanorod arrays to transport photogenerated electrons, with low recombination losses, to the back-contact relatively efficiently.

Fig. 6 gives the photocurrent–voltage curves of the dye-sensitized ZnO electrodes, while the photoelectrochemical properties of these electrodes are listed in Table 1. Under the illumination of simulated solar light (42 mW/cm^2) from 150 W Xe lamp, a sandwiched-type solar cell, which is fabricated with N3-sensitized ZnO nanorod arrays photoanode, 0.5 mol/L LiI/0.05 mol/L I_2 PC electrolyte, and a Platinized ITO glass counter electrode, was used to study the characteristics of these electrodes. The overall yield (η) is expressed by the following equation:

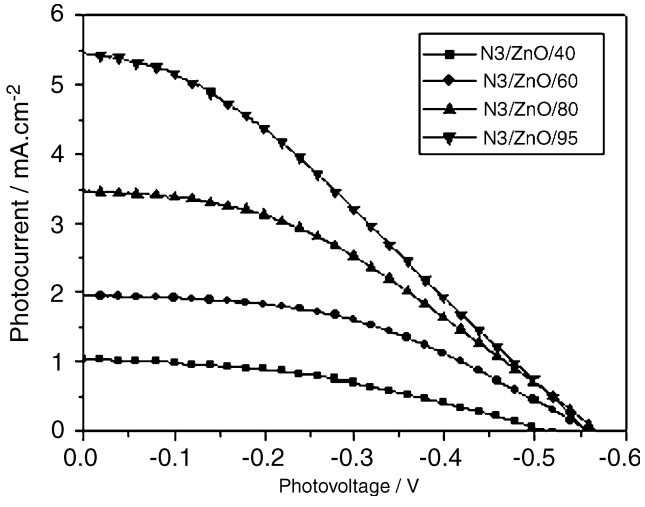

Fig. 6. Photocurrent–voltage curves of the N3-sensitized ZnO electrodes grown from 95 to 40 °C.

Table 1
Parameters of solar cell based on dye-sensitized ZnO nanorod arrays films at different growth temperatures from 95 to 40 °C

Growth temperature (°C)	I_{sc} (mA/cm^2)	V_{oc} (V)	FF	η (%)
40	1.02	0.52	0.39	0.5
60	1.96	0.56	0.42	1.1
80	3.46	0.57	0.38	1.8
95	5.18	0.55	0.36	2.4

$$\eta = (V_{oc} I_{sc} \mathrm{FF})/P_{in}, \quad (2)$$

$$\mathrm{FF} = V_{opt} I_{opt}/V_{oc} I_{sc}, \quad (3)$$

where P_{in} is the power of incident white light, FF is fill factor, V_{opt} and I_{opt} are voltage and current for maximum power output, and V_{oc} and I_{sc} are open-circuit photovoltage and short-circuit photocurrent, respectively. We can see from Fig. 5 and Table 1 that the maximum overall energy conversion efficiency, 2.4%, was achieved in dye-sensitized N3/ZnO/95 solar cell compared to those of the dye-sensitized N3/ZnO/80, N3/ZnO/60 and N3/ZnO/40 systems, respectively. It is well known that the photoconversion efficiency increases, in a certain range, with the increasing of nanocrystalline film thickness because thicker films provide larger amount of absorbed dyes and more photon-capturing changes. The overall yield obtained in our experiments is quite close to that of the solar cells based on ZnO nanoparticle films with a thickness of 7–9 μm under the same conditions [18]. However, when considering the facts that the thickness of ZnO film used in our experiments is only 1.9 μm, it may be concluded that the photo-to-electric conversion efficiency of the dye-sensitized ZnO nanorod arrays electrode is much higher when the film thickness is the same. Solar cell based on N3/ZnO/40 electrode has the lowest short-circuit photocurrent and overall yield, though the lowest values are still higher than that of the solar cells based on ZnO nanoparticle films with the same thickness, due to its thinnest film thickness among the four electrodes.

The relatively high efficiency observed for ZnO nanorod array films can be ascribed to the as-synthesized film nanostructure. Since every ZnO nanord is a single crystal that can provide electron transportation channel to the conducting substrate, and the as-

prepared nanorod arrays have high porosity and large surface area which would be beneficial for adsorbing more dyes to improve the light harvest efficiency. Furthermore, the photogenerated electrons can transport directly through the oriented nanorods to the conducting substrates. This greatly reduces the recombination losses of the photogenerated charge-carriers due to fewer grain boundaries in charge transportation process. The preparation of thicker ZnO nanorod array films and the study of their photoelectrochemical properties are in progress in our group.

4. Conclusion

Well-aligned and diameter-controlled single-crystalline ZnO nanorod arrays have been prepared at different growth temperatures and used as photoanode in Grätzel-type solar cell. Relatively high photoconversion efficiency has been obtained with rather thin ZnO films, which suggests that thicker ZnO nanorod array films might result in much higher overall conversion efficiency. The preparation of thicker ZnO nanorod array films and the study of their photoelectrochemical properties are in progress in our group.

Acknowledgments

The authors gratefully acknowledge the support from the National Natural Science Foundation of China (No. 20073003) and the support from USTB.

References

[1] M.H. Huang, S. Mao, H. Feick, H. Yan, Y. Wu, H. Kind, E. Weber, R. Russo, P. Yang, Science 292 (2001) 1897.
[2] J. Zhong, A.H. Kitai, P. Mascher, W. Puff, J. Electrochem. Soc. 140 (1993) 3644.
[3] N. Beermann, L. Vayssieres, S.-E. Lindquist, A. Hagfeldt, J. Electrochem. Soc. 147 (2000) 2456.
[4] N. Yamazoe, Sensors Actuators B 5 (1991) 7.
[5] G.S. Trivikrama Rao, D. Tarakarama Rao, Sensors Actuators B 55 (1999) 166.
[6] J.-J. Wu, S.-C. Liu, Adv. Mater. 14 (2002) 215.
[7] J.-J. Wu, S.-C. Liu, J. Phys. Chem. B 106 (2002) 9546.
[8] K. Govender, D.S. Boyle, P. O'Brien, D. Binks, D. West, D. Coleman, Adv. Mater. 14 (2002) 1221.
[9] D.S. Boyle, K. Govender, P. O'Brien, Chem. Commun. (2002) 80.
[10] S. Yamabi, H. Imai, J. Mater. Chem. 12 (2002) 3773.
[11] L. Vayssieres, Adv. Mater. 15 (2003) 464.
[12] L.E. Greene, M. Law, J. Goldberger, F. Kim, J.C. Johnson, Y. Zhang, R.J. Saykally, P. Yang, Angew. Chem. Int. Ed. 42 (2003) 3031.
[13] M. Grätzel, Prog. Photovolt. Res. Appl. 8 (2000) 171.
[14] M. Guo, P. Diao, S.M. Cai, J. Solid State Chem. 178 (2005) 1864.
[15] L. Vayssieres, K. Keis, S.-E. Lindquist, A. Hagfeldt, J. Phys. Chem. B 105 (2001) 3350.
[16] M. Guo, P. Diao, S.-M. Cai, Acta Chim. Sinica 61 (2003) 1165.
[17] M. Guo, P. Diao, S.M. Cai, Appl. Surf. Sci. 249 (2005) 71.
[18] H. Rensmo, K. Keis, H. Lindstrom, S. Sodergren, A. Solbrand, A. Hagfeldt, S.E. Lindquist, L.N. Wang, M. Muhammed, J. Phys. Chem. 101 (1997) 2598.